PROGRESS IN COLOR, COLORANTS AND COATINGS

available online @ www.pccc.icrc.ac.ir

Progress in Color Colorants Coating 18 (2025), 343-361

Ministry of Science, Research and Technology
Institute for Color Science & Technology

Prevention of TiO_2 Crowding through Steric Hindrance by Silane Coupling in Organic Coatings

A. Ödev, O. Uzunkavak*
Chemical Engineering Department, Faculty of Engineering, Ege University, 35100 Bornova Izmir – Türkiye

ARTICLE INFO

Article history:
Received: 13 Nov 2024
Final Revised: 03 Mar 2025
Accepted: 05 Mar 2025
Available online: 15 Apr 2025

Keywords:
Hiding power
Light scattering
Organic coatings
Silane coupling
Steric hindrance
Titanium dioxide

ABSTRACT

This study aimed to reduce TiO_2 crowding through steric hindrance by grafting 3-methacryloxypropyltrimethoxysilane (MPS) onto the pigment surface. This was achieved using various TiO_2/MPS mass ratios in dispersion formulations and characterized by FTIR and TGA analyses. Characterizations revealed the most efficient grafting for the TiO_2/MPS ratio of 100/10 (labeled TT3). An optimum particle size of 250-350 nm for opacity was obtained after 30 minutes of TT3 dispersion, resulting in the maximum number density of 47.45 % within this size range. The TT3 dispersion demonstrated high lightness and opacity, with minimal changes in surface properties compared to untreated and other MPS-grafted TiO_2 dispersions, suggesting its advantageous use. The impact of pigment volume concentration (PVC) on pigment spacing was examined using topcoats with PVC levels of 7, 11, and 13 %, incorporating TT3 and untreated TiO_2 dispersions. The lightness and opacity results indicated that lower PVC levels allowed wider spacing between pigment particles in dry films. Additionally, untreated TiO_2 pigments exhibited increased crowding at equivalent PVC levels compared to the TT3 dispersion, while a rise in PVC did not diminish opacity or lightness in dry films with TT3, highlighting the even pigment distribution. Notably, dry films of the topcoats with TT3 or untreated pigment dispersions revealed that the TT3-containing topcoat at 30 µm for a given PVC exhibited almost identical properties to those of the topcoat containing untreated TiO_2 dispersion at 55 µm. Thus, MPS grafting facilitated reduced pigment usage in paint formulations and lower paint consumption per unit area, decreasing volatile organic compound emissions. Prog. Color Colorants Coat. 18 (2025), 343-361© Institute for Color Science and Technology.

1. Introduction

Dry pigments, made up of aggregates or agglomerates through cohesive forces such as hydrogen bonding, ion-dipole, and dipole-dipole interactions, have to be crushed into their primary particles when they are dispersed in the carrier, which includes the binder, additives, and solvents. Film formation occurs after pigmented paint is applied to a substrate and cured [1, 2]. The applied film shrinks during this process, and the distance between the pigment particles decreases. The opacity of a dry film containing white pigments is achieved by scattering visible light from the surface of the coating and/or backscattering visible light as it passes through the film before reaching the substrate [3]. White pigments interact with light on the surface, changing the light beam's direction. This is called light scattering; its mechanisms are reflection, refraction, and diffraction.

*Corresponding author: * onuruzunkavak@gmail.com
https://doi.org/ 10.30509/pccc.2025.167429.1345

Titanium dioxide (TiO_2) pigments are ubiquitous in the paint industry due to their unique ability to scatter visible light. TiO_2 is used in virtually every organic coating except those that are clear or entirely black. This allows for light-colored and white paints by providing opacity without resorting to light absorption [4]. In single-pigmented white coatings comprising TiO_2, augmenting pigment loading can boost hiding power. However, beyond a specific loading, crowding occurs as pigment particles overlap due to the limited interparticle spacing, and the overall scattering surface area is diminished [3, 4]. Many experimental studies performed over the last four decades revealed that TiO_2 particle spacing was completely indifferent to the presence of extender particles that are no larger than the TiO_2 particles themselves, and very large extenders worsened the degree of TiO_2 dispersion, as expected, due to crowding [4, 5].

Diffraction of light highly depends on particle size and size distribution of particles. If particles are too large or closely spaced, little diffraction occurs [6]. On the other hand, if the pigment particles are too small, the light will not be affected by the particle volume, and diffraction will again be low. For higher diffraction efficiency, the particle size of pigments should be comparable to the wavelength of incident light, and scattering volumes should not be overlapped. The visible light spectrum ranges between 400 and 700 nm wavelengths, with an average of 550 nm. For the most efficient scattering, particle size should be around half of the wavelength of incident light [3, 7]. Therefore, the optimum particle size of dispersion is around 250-350 nm for efficiently using TiO_2.

On the other hand, spacing between particles is an important parameter for optimum scattering efficiency. Thiele and French used the finite element method to calculate the optimum spacing between TiO_2 particles [6]. Accordingly, the maximum scattering for rutile TiO_2 in an acrylic medium would be with particles of 250-350 nm in size with 400 nm spacing.

The solid content in paint formulations highly influences the film's surface leveling, gloss, mechanical strength, and integrity [8]. Pigment Volume Concentration (PVC) is the fractional volume of non-film forming particles (pigments and, if present, fillers) in the total solid volume of the dry paint film (binders, pigments, fillers). There is a critical value for PVC called Critical Pigment Volume Concentration (CPVC). The binder is sufficient to provide a fully adsorbed layer on the pigment surfaces and fill the gaps between the pigment particles at this value [9]. PVC is calculated according to equation 1, where $V_{Pigments}$ is volume of pigments, $V_{Fillers}$ is volume of fillers, and $V_{Binders}$ is the volume of binders. CPVC is calculated according to equation 2 from the oil absorption of pigments, which is expressed as grams of linseed oil sufficient to fill the interstices between pigment particles per 100 g of pigment and the density of pigments.

$$\text{PVC, \%} = \frac{\sum V_{Pigments} + V_{Fillers}}{\sum V_{Pigments} + V_{Fillers} + V_{Binders}} \times 100 \quad (1)$$

$$\text{CPVC, \%} = \frac{1}{1 + \sum(\text{Oil Absorption}_{Pigments})(\rho_{Pigments})/93.5} \times 100 \quad (2)$$

To a certain extent, PVC values lower than CPVC are optimal for paint formulations [10]. As PVC increases, the paint film's permeability and the metal substrate's corrosion risk increases. Therefore, CPVC should not be exceeded. When there is excess resin, PVC is well below CPVC, and the film has low permeability, which will prevent corrosion. However, blistering may occur below a certain PVC value when absorbed water cannot escape from the dry film.

Surface modification and silane coupling on TiO_2 particles have been investigated for years. These studies were accelerated in recent years to improve TiO_2 properties in various application areas. Pigment manufacturers treat surfaces of commercial TiO_2 pigments with Al_2O_3, SiO_2, and ZrO_2 for better dispersibility and UV and weathering resistance [11, 12]. Therefore, silane compounds cannot directly interact with TiO_2 during surface modification; silanization occurs between silane compounds and the surface treatment of TiO_2 pigment. Organic compounds consisting of at least one silicon bond (C–Si) are called organosilane. They have an organic group chain and a hydrolyzable group so that they can be used as molecular bridges between the organic medium of a coating and the inorganic surface of pigments [13]. Silanization can be summarized as a process involving hydrolysis and condensation [14, 15]. Hydrolysis of silicon-containing parts to form silanol groups is the first step, which involves introducing organosilane compounds into a hydroxyl-containing medium like alcohol. Then hydrogen bonding occurs between the $–OCH_3$ groups of silane and –OH groups of the inorganic surface. The second step is condensation, where Si–O–Si and Al–O–Si bond formation occurs on

the inorganic pigment surface with the loss of H_2O molecules. After the hydrolysis of silanol groups, they will condense with each other and form a polymeric siloxane [16].

Siddiquey et al. modified commercial TiO_2 with metharyloxypropyltrimethoxysilane (MCPTMS) and found that the photocatalytic activity of TiO_2 was reduced [17]. Sabzi et al. modified TiO_2 nanoparticles with aminopropyltrimethoxysilane (APS) to improve dispersibility, mechanical properties, and UV resistance [18]. In another study, Zhao et al. examined the modification of TiO_2 with 3-isocyanatopropyltri methoxysilane (IPTMS) and 3-aminopropyltrimethoxy silane (APTMS) using an aqueous process [19]. Grafting efficiency was higher for IPTMS due to the high reactivity of isocyanate groups (NCO) to silanol groups (R_3SiOH). However, there is no study in the literature in which silane coupling was performed to reduce the crowding of TiO_2 pigment particles. Additionally, there is no study on silane coupling of 3-methacryloxy propyltrimethoxysilane (MPS) on TiO_2 pigments.

As the methacrylate group in MPS is not a chromophore, it is also expected to be colorless and transparent when grafted onto the TiO_2 surface to ensure white topcoats. Also, MPS is renowned for its high potential for forming long chains, which makes MPS coupling a suitable candidate as a spacer. This study aimed to maximize the light scattering capabilities of commercial TiO_2 pigments by averting pigment crowding through steric hindrance facilitated by MPS coupling on pigment particles. Isobutyl alcohol was used for the hydrolysis of MPS. TiO_2 particle size distribution and silane coupling treatment on TiO_2 surfaces were optimized to increase scattering. TiO_2 to MPS mass ratio was varied in dispersion formulations to characterize the grafting efficiency by FTIR and TGA analyses. The effect of TiO_2 to MPS mass ratio and duration of pigment dispersion on the white topcoat properties was investigated with different dry film thicknesses. Color, hiding power, and surface properties were compared. The effect of PVC on topcoats' pigment spacing and corrosion resistance was examined. Consequently, the research aspired to design high opacity topcoats compared to conventional TiO_2-containing topcoats by less pigment loading, thus paving the way for reduced paint consumption per unit surface area by achieving the desired color and hiding properties with thinner dry film layers, curbing VOC emissions into the environment. The commercialization potential of the research results is substantial, as the paint manufacturers are constantly seeking environment-friendliness and sustainability, and the regulations attempt to reduce VOC emissions from industrial activities, including the paint and coating industry.

2. Experimental

2.1. Materials

The rutile crystal form of TiO_2 pigment was supplied with the trade name Kronos 2310 (Kronos International Inc., Leverkusen, Germany). The supplied pigment has a surface treatment with aluminum, silicon, and zirconium compounds and organic substances. The supplier declares the primary particle size (d50), surface area, and oil absorption value of the pigment as 0.20 μm, 12-16 m^2/g, and 14-17 g/100 g pigment. Zirconium oxide grinding beads with a 1.4-1.6 mm diameter were purchased for use in the dispersion machine (Netzsch - Feinmahltechnik GmbH, Selb, Germany). 3-methacryloxypropyltri methoxysilane (MPS) as the silane coupling agent was purchased with the trade name Silquest A-174NT (Momentive Performance Materials Inc., Niskayuna, NY, USA). Acrylic resin, solvents, bentonite paste, and aliphatic polyisocyanate (hardener) were generously provided by Kansai Altan Boya Sanayi A.Ş.

2.2. Experimental setup

2.2.1. TiO_2 pigment dispersion

Pigment powders form aggregates and agglomerates due to pressure and moisture during storage and transportation. To break these structures and return the pigments to their original particle sizes, grinding media must apply forces such as impact, shear, and attrition during the dispersion process. Zirconium oxide (ZrO_2) has a high hardness, which allows it to effectively break up aggregates and agglomerates of pigments during the dispersion process without significant wear, and it is chemically inert, meaning it is unlikely to react with TiO_2 pigment or introduce contaminants that could alter the properties of the dispersion [1, 2]. Pigment powders in the form of aggregates and agglomerates were dispersed in the disperser with ZrO_2 beads with a 1.4-1.6 mm diameter. This size provides an optimal balance between surface area and the mechanical energy for effective dispersion. Smaller beads, less than 1 mm, can generate more shear force but may cause excessive wear and require more energy. On the other hand, larger beads greater than 2 mm are

less effective at breaking up fine pigment aggregates and result in a slower dispersion process [1, 2]. The duration of this process was optimized to reach the desired particle size of 250-350 nm and the highest number of particles in this size range. Particle size and size distributions of pigment dispersions were measured on the day they were prepared to avoid inconvenient results due to re-agglomeration.

2.2.2. Surface modification of TiO_2 by silane coupling

Surface modification of TiO_2 was performed during the dispersion process. For the silane coupling reaction, MPS was hydrolyzed in isobutyl alcohol (IBA) and TiO_2 powder was added directly to the solution. The number of hydroxyl groups needed for complete hydrolysis was calculated based on the number of MPS molecules present to determine the required amount of IBA. Since each MPS molecule contains three hydrolysable groups, the number of IBA molecules required was three times that of MPS molecules (Figure 1). This ensures that every hydrolysable group on the MPS molecules can undergo hydrolysis and form silanol groups, which then react with the TiO_2 surface to achieve proper surface modification.

The amount of MPS in the formulations was converted into the number of molecules by dividing the amount by its molecular weight (MW_{MPS} = 248.35 g/mol) and multiplying by Avogadro's number (6.02214076×10^{23} mol^{-1}). The amount of IBA was then calculated by multiplying the number of MPS molecules by three and converting the resulting number to mass using the molecular weight of IBA (MW_{IBA}: 74.12 g/mol) and Avogadro's number (Table 1). On the other hand, the amounts of IBA and TiO_2 were kept constant to keep other variables, such as the degree of wetting, stable. IBA to TiO_2 ratio was determined through empirical testing as 20 w/w %, meaning 20 g IBA for every 100 g of TiO_2, to ensure complete hydrolysis of MPS of all levels and effective wetting of TiO_2 particles. This way, TiO_2 particles were evenly distributed and readily available for the coupling reaction with MPS. MPS content in the samples was altered to specify the optimum TiO_2/MPS ratio for grafting efficiency. The MPS-coupled pigment samples were denoted as TT1, TT-2, TT-3, and TT-4 with increasing MPS content (2.5, 5, 10, 20 g MPS per 100 g of pigment) and the untreated sample as UT. The viscosities of samples varied due to the different amounts of MPS in the liquid form. Samples grafted with different TiO_2/MPS ratios were characterized to determine their grafting efficiency. Before the TGA characterization, the MPS-coupled samples were washed 3 times with tetrahydrofuran (THF) to remove unreacted free MPS. The particles were then dried at 120 °C for 1 hour.

Table 1: Determination of the IBA amount based on the hydroxyl groups required for the hydrolysis of MPS.

Property	TT1	TT2	TT3	TT4
TiO_2 amount in formulations (g)	100	100	100	100
MPS amount in formulations (g)	2.5	5	10	20
Number of MPS molecules*	6.06E+21	1.21E+22	2.42E+22	4.85E+22
Required number of IBA molecules*	1.82E+22	3.64E+22	7.27E+22	1.45E+23
Required amount of IBA (g)	2.24	4.48	8.95	17.91
IBA amount in formulations (g)	20	20	20	20

* MW_{MPS}: 248.35 g/mol; MW_{IBA}: 74.12 g/mol

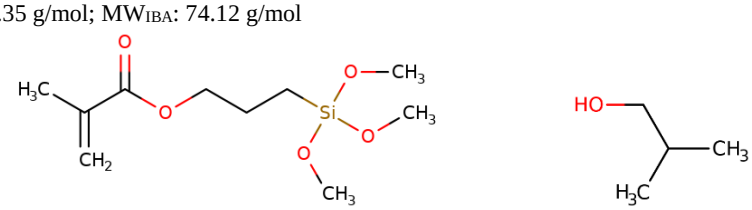

a) **b)**

Figure 1: Molecular structure of a) MPS and b) IBA.

Pigment, MPS and IBA were stirred for 15 minutes with a high shear Cowles-type impeller for homogenization. Then, acrylic resin and bentonite paste were added to the system and dispersed with the disperser machine. The investigated parameters and their levels are listed in Table 2, which are TiO_2 to MPS ratio, dispersion time, PVC, and dry film thickness. These parameters were determined based on early-stage experiments.

Table 2: Investigated parameters and their levels.

Parameters	Levels
TiO_2 to MPS ratio	100/0; 100/2.5; 100/5; 100/10; 100/20
Dispersion time	30 min; 45 min
PVC	7%; 11%; 13 %
Dry Film Thickness (DFT)	30 μm; 55 μm

2.3. Characterization of TiO_2 pigment

2.3.1. Particle size and particle size distribution

A laser diffraction technique was used to determine the particle size and size distribution. Measurements were made using a Mastersizer 3000 with a Hydro EV unit (Malvern Panalytical, Worcestershire, UK). This equipment operates with the Dynamic Light Scattering (DLS) method. A glass cuvette was used for measurements and stirred at 1800 rpm. Ultrasound was not applied. Particle size distributions were obtained regarding volume, number, and surface area. Average particle size calculations are given in equations 3 to 5 [20], where v_i is the fraction of a class of particles and D_i is the diameter of each class.

$$D[1,0]=\frac{\sum_{i=1}^{n} D_i v_i}{\sum_{i=1}^{n} v_i} \quad (3)$$

$$D[3,2]=\frac{\sum_{i=1}^{n} D_i^3 v_i}{\sum_{i=1}^{n} D_i^2 v_i} \quad (4)$$

$$D[4,3]=\frac{\sum_{i=1}^{n} D_i^4 v_i}{\sum_{i=1}^{n} D_i^3 v_i} \quad (5)$$

Based on the assumption that the particles are perfect spheres, the mean diameter can be calculated from the mean volume and the volume of the sphere equation.

2.3.2. Thermogravimetric analysis (TGA)

Thermogravimetric analysis (TGA) was used to measure the mass of a sample as a function of temperature and time. A TGA-SDT Q600 (TA Instruments, New Castle, DE, USA) equipment was used, and the samples were heated from 20-900 °C at a rate of 10 °C/min. Analyzes were performed under nitrogen; the gas flow rate was 50 mL/min. The degree of weight loss indicated the effectiveness of the MPS grafting onto the TiO_2 surface.

2.3.3. Fourier transform infrared spectroscopy analysis (FTIR)

Fourier Transform Infrared Spectroscopy (FTIR) (PerkinElmer Inc., Hopkinton, MA, USA) analysis was performed using the KBr pellet method to characterize the treated TiO_2 samples and the identification of the fingerprint region of the material. Chemical bonds formed by silane coupling were investigated between 4000 to 450 cm^{-1} wavenumbers. The spectra of MPS-coupled TiO_2 samples were compared with that of untreated TiO_2.

2.3.4. Scanning electron microscopy analysis (SEM)

Scanning electron microscopy (SEM) (Carl Zeiss AG, Jena, Germany) was employed to investigate and compare spatial pigment distribution within the topcoat paint films. Steel plates were coated with topcoats having a dry film thickness of 30 μm, and images were captured from the lateral sections to analyze the pigment crowding effects.

2.4. Characterization of topcoat properties

The prepared TiO_2 dispersions were incorporated into a topcoat formulation in varying amounts. The solvent-borne 2K PUR system was the experimental coating system; the reactive components, such as hydroxyls and isocyanates, existed separately. While the pigmented component was the acrylic resin with a hydroxyl group, the clear component was the hardener with an isocyanate group. The topcoat was applied to the substrate using an automatic spray robot (RX20-D, Amsterdam, Netherlands) and cured at 80°C for 30 min to form a film.

2.4.1. Color properties

The light source, object, and observer influence the perception of color. International Commission on Illumination (Commission International de l'Eclairage - CIE) established CIE L*a*b* color space to represent color with a mathematical model. The model represents a spherical space, where the lightness value cannot be negative but runs from 0 (black) to 100 (white); that is, as L* increases, the color becomes lighter. On the other hand, a* is the green (-ve) to red (+ve), and b* is the blue (-ve) yellow (+ve) axis.

The difference between two colors (ΔE) can be calculated based on their distance, as they are two points in a three-dimensional space. In equation 6, "ΔL*" is the difference on the lightness axis, "Δa*" is the difference on the green/red axis, and "Δb*" is the difference on the blue/yellow axis.

$$\Delta E = \sqrt{\Delta L^{*2} + \Delta a^{*2} + \Delta b^{*2}} \quad (6)$$

In this study, a specular component included (SCI) measurement mode of Color i5 spectrophotometer with a D65 illuminant and 10-degree observer (X-Rite, Regensdorf, Switzerland) was used together with Color iQC software according to ISO 7724-3:1984 for color characterization [21].

2.4.2. Hiding power

Hiding power or opacity is the ability of a coating to cover a substrate, which can be measured by contrast ratio (CR %) analysis. Fresh paints were applied on black and white opacity cards and allowed to dry overnight. Luminance (Y) values were obtained with visible spectroscopy (X-Rite, Regensdorf, Switzerland) to calculate CR % values according to equation 7. If the Y values measured on the black and white backgrounds are identical, the CR % is 100, and the resulting color is not affected by the color of substrate. However, coatings with a CR % value greater than 98 % are considered opaque [3].

$$\text{CR } \% = \frac{Y_{black}}{Y_{white}} \times 100 \quad (7)$$

2.4.3. Gloss and surface leveling

The term gloss defines the smoothness of a coating surface. In other words, as surface roughness increases, the gloss of a coated surface decreases. The intensity of specular reflection, brightness, distinctness of image, and haze influence gloss. Gloss measurements were made at 20° and 60° incidence angles. Microstructures on the surface cause scattering at different angles from specular reflection, which is called haze. Haze values are measured at ±1.8° lateral angles of the reflected light at 20°. The distinctness of the image (DoI) is also related to the smoothness of the surface. When the image of an object is projected onto the coated surface, the surface roughness affects the mirror image's resolution. If the surface of the coated surface is not perfectly smooth, then the incident light will not be reflected at the mirror angle [8]. Gloss, haze and DoI were measured with a Rhopoint IQ instrument (Rhopoint Instruments, East Sussex, UK) to investigate the effect of pigment particle size and distribution and amount of the silane coupling agent on surface leveling.

2.4.4. Corrosion resistance

The corrosion resistance of white topcoats was investigated using salt spray experiments. Topcoats were applied on previously primed cold rolled steel plates. The coated sides of the plates were then X-cut to be placed in a salt spray chamber (Ascott Analytical Equipment, Tamworth, UK). They were subjected to atomized salt solution (5 % aqueous sodium chloride solution) in the chamber at 18-23 °C temperature, 4-6 bar pressure, and 45-85 % relative humidity conditions according to ASTM B117 [22]. Test results were screened after 1000 hours, and the frequency and size of blistering and rust progressions were compared. Blisters were classified according to ASTM D714 [23].

3. Results and Discussion

3.1. Determination of the ideal number of particles for light scattering

Recent studies show that for maximum scattering efficiency, the particle size of TiO_2 pigment should be 250-350 nm, and the particles should be a minimum of 400 nm apart in an acrylic medium. This model can be represented as given in Figure 2 for two neighboring particles. Löf et al. revealed that the dispersion state of TiO_2 in acrylic resin does not change during drying [7]. Therefore, the optical properties were determined analytically by the wet paint design.

A model was derived to obtain the ideal number of particles for a specific volume (Figure 2). Average particle diameter and effective radius, including spacing, were taken as 300 and 350 nm, respectively. The density of TiO_2 pigment is 4 g/cm^3, and the

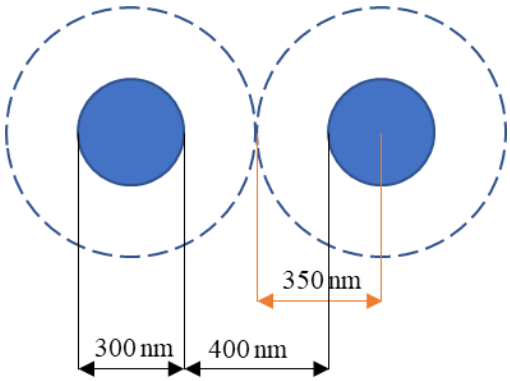

Figure 2: Schematic view of two neighboring TiO_2 particles for maximum scattering.

volume of 100 g pigment is 25 cm^3. According to the model, the effective volume is calculated as 0.18 μm^3, assuming that the particles of 300 nm diameter should be 400 nm apart for maximum scattering efficiency. The number of particles in a 100 g sample will be then 1.4E+14. Suppose these particles are evenly distributed over 1 m^2 area with a dry film thickness of 30 µm and 55 µm. In that case, the number of particles that can fit in the calculated application volume for maximum scattering (volume of application divided by effective volume of one particle) will be 1.7 E+14 and 3.1 E+14, respectively (Table 3).

3.2. Surface modification of TiO_2 by silane coupling

3.2.1. Characterization of treated TiO_2 particles

3.2.1.1. Determination of grafting with FTIR

FTIR spectroscopy was used to confirm the grafting of MPS onto TiO_2 particles. Covalent bond formation in the form of Si–O–Si and Al–O–Si bonds is expected between the siloxane group of MPS and the Al_2O_3 and SiO_2 treatment on the TiO_2 pigment surface as a result of the condensation step of silylation reaction.

The spectra of pure MPS molecules, untreated pigment particles, and treated pigment particles were compared to elucidate the spectral shifts of bond formations due to silane coupling. (Figure 3). The peak at 1380 cm^{-1} often corresponds to C-H bending in methyl groups, and the peak at 1630 cm^{-1} is typically associated with the C=C stretch (carbon-carbon double bond stretch) for all samples [24]. A strong peak is seen at 1720 cm^{-1} for the sample of pure MPS, corresponding to the C=O stretching vibration band [16, 25]. The stretching vibration corresponding to carbonyl groups was shifted to lower wave numbers for the treated samples by the hydrogen bond formation between the carbonyl groups of MPS and hydroxylic groups of the inorganic TiO_2 surface [16, 26]. The peaks at 1705, 1704, 1716, and 1717 cm^{-1} for the treated samples TT1, TT2, TT3, and TT4, respectively, indicate gradual grafting of MPS molecules onto TiO_2 particles. On the other hand, the untreated TiO_2 sample did not demonstrate any peaks at the wavenumbers from 1696 to 1722 cm^{-1}.

3.2.1.2. Determination of grafting efficiency by TGA analysis

Thermogravimetric analysis (TGA) provides information on the surface treatment efficiency of inorganic particles based on temperature-dependent weight differences. Treated and untreated TiO_2 samples were heated from 20°C to 900 °C at 10 °C/min. The TGA curves at percent weight loss as a function of temperature based on the TiO_2/MPS ratio are shown in Figure 4a.

Table 3: Determination of the ideal number of particles.

Average particle diameter, nm	300
Effective particle radius, nm	350
Volume of 1 particle, μm^3	0.01
Effective volume of 1 particle, μm^3	0.18
Number of particles in 100 g of sample	1.4 E+14
Volume of application area (1 m^2, 30 µm DFT), μm^3	3.0 E+13
Number of particles in the application volume (30 µm DFT)	1.7 E+14
Volume of application area (1 m^2, 55 µm DFT), μm^3	5.5 E+13
Number of particles in the application volume (55 µm DFT)	3.1 E+14

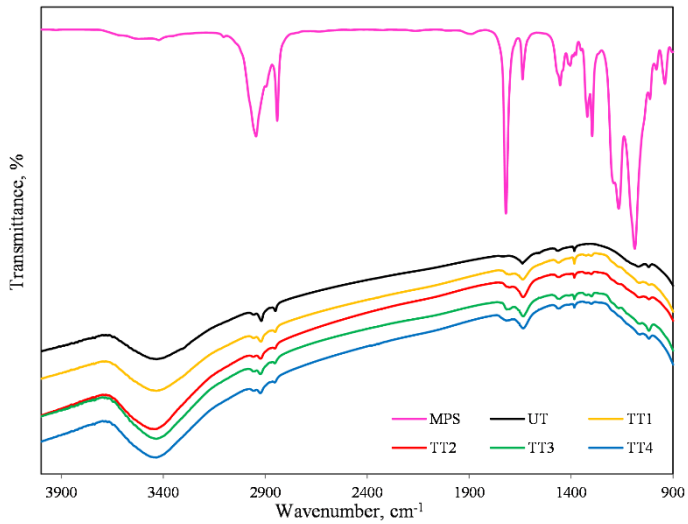

Figure 3: FTIR spectra of MPS, untreated and treated particles.

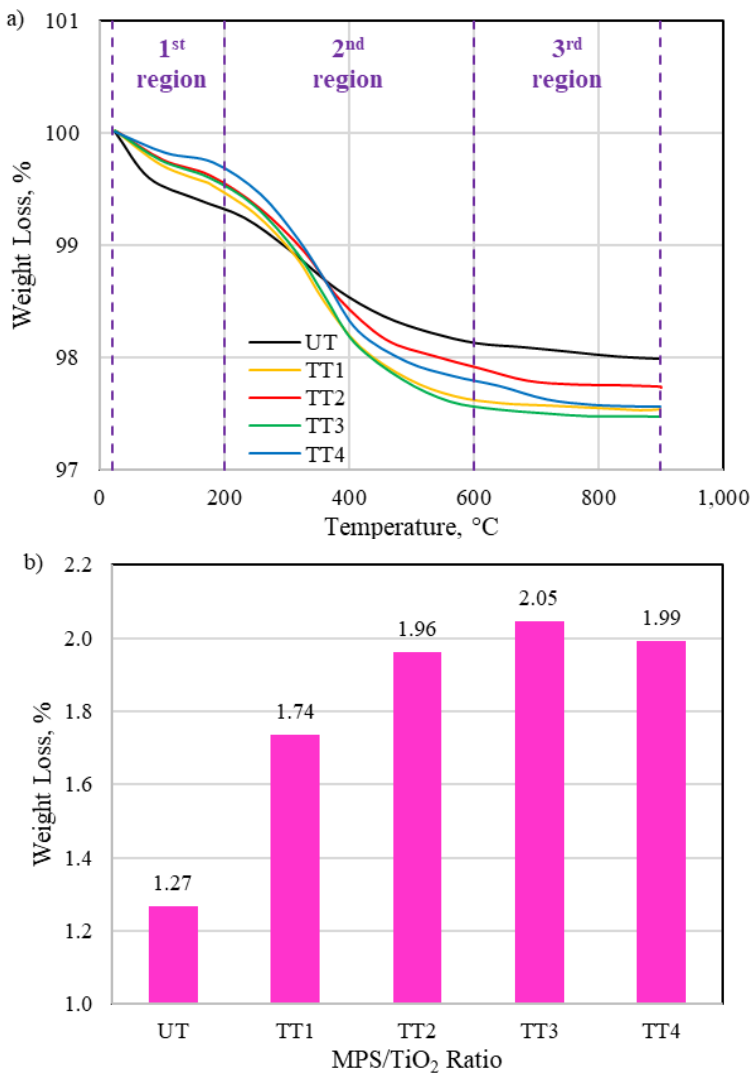

Figure 4: Results of TGA analysis: a) percent weight loss as a function of temperature, b) percent weight loss as a function of TiO_2/MPS ratio.

Three regions (20-200, 200-600, and 600-900 °C) can be distinguished in the weight loss curves. The first region for the MPS-coupled TiO_2 samples is attributed to the loss of loosely adsorbed silane groups. Since loosely adsorbed and free MPS molecules were washed away with tetrahydrofuran (THF) after silane coupling, weight losses in this region were less than 0.6 % for all samples. The weight loss in the second region corresponds to the MPS coupling on the surface, and the third region indicates the self-condensation of the silane. Similarly, Liu et al. described these regions in their work on silanization of fumed silica [27]. They reported a certain amount of weight loss in the first region, which might lie in how effectively their silane coupling was performed, resulting in higher losses. Also, their second weight loss region was attributed to the coupling of MPS to the silica surface, which followed a comparable trend with this study. They also described a small weight loss in the third region as the condensation of surface silanol.

The more significant weight loss observed in the untreated TiO_2 samples in the first region is likely due to the thermal decomposition of the remnant solvent on the surface. In contrast, the overall decomposition of the untreated TiO_2 is the lowest among all the samples, indicating that it is relatively stable in nitrogen [28].

The percent weight loss in the second region, depending on the TiO_2/MPS ratio, is shown in Figure 4b. Weight loss percentages are also detailed in Table 4 concerning the individual weight loss regions. The highest weight loss was observed at temperatures between 200 and 600 °C, and the percent weight loss increased with an increase in MPS content up to the TiO_2/MPS ratio of 100/10, indicating an efficient grafting for the TT3 sample. The highest weight loss in the self-condensation region was experienced with the highest MPS ratio (100/20) of the TT4 sample, indicating an excess presence of MPS in its formulation. Figure 4b also reveals the highest grafting efficiency was obtained with the TiO_2/MPS ratio of 100/10 (TT3).

3.2.2. Optimization of dispersion time to achieve optimum particle size

Experiments were conducted using the TT3 formulation to determine the dispersion time required to achieve the optimum particle size of 250-350 nm. Pigment dispersions were prepared and processed for various durations: 15, 30, 45, 90 and 135 minutes, 3 and 6 hours. These dispersions were processed in a closed, constant-volume mill base to minimize the influence of external variables. The optimum dispersion time was identified based on particle size measurements.

Each experimental condition was replicated twice on separate days under identical settings to ensure consistency in particle size distribution across different batches. This repetition enabled reliable reproducibility, as the average particle sizes from each batch showed no significant differences. The numerical results presented in this section correspond to the first batch group. Particle size distributions (PSD), expressed as intensity (Figure 5), exhibit the percentage of particles by number. The hatched area in Figure 5 is the 250-350 nm region, which is the optimum particle size range for maximum scattering. The maximum particle accumulation in this region was obtained at 15, 30, and 45 minutes of dispersion times. Since the particles shifted to coarser sizes with the 15 minute dispersion time, the 30 and 45 minute dispersion times samples were selected for further investigation.

Table 4: Percent weight loss obtained by TGA analysis.

Sample	Weight Loss, %			
	20-200 (°C)	200-600 (°C)	600-900 (°C)	Total
UT	0.538	1.266	0.156	1.960
TT1	0.335	1.737	0.172	2.240
TT2	0.337	1.963	0.098	2.400
TT3	0.342	2.046	0.092	2.480
TT4	0.215	1.991	0.217	2.420

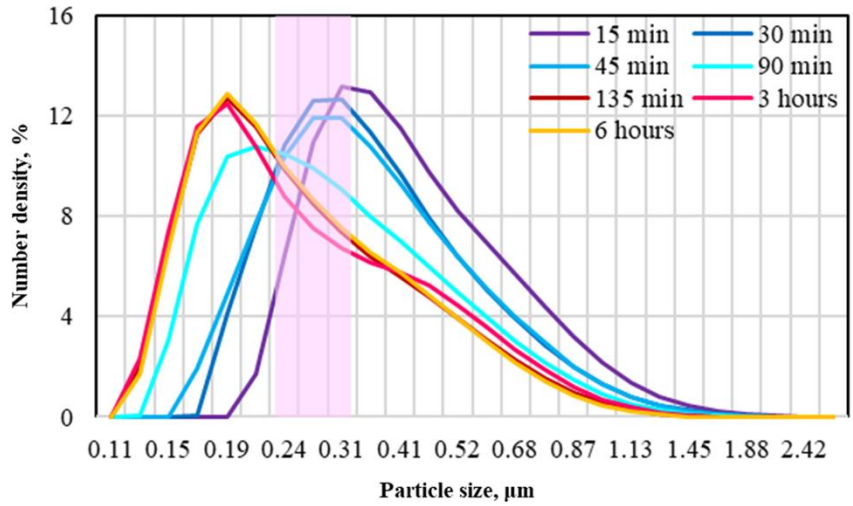

Figure 5: PSD of dispersions obtained with different durations in terms of intensity.

The average particle sizes of the samples, D(avg), were calculated using the volume average equation. With increased dispersion duration, the particles were exposed to shear, compression, and impact forces for a longer period, and the particle sizes decreased. The highest number of particles in the optimum size range (250-350 nm) was obtained with 30 min dispersion by 47.45 % (Table 5).

3.2.3. Effect of silane coupling on white topcoat properties

The effect of silane coupling on the white topcoat properties was investigated. Pigment dispersions were prepared in IBA with varying TiO_2/MPS ratios, and silanization was accomplished simultaneously. Paint preparation was then performed with the addition of complimentary paint components to this mixture. The amount of ingredients, such as TiO_2 pigment, acrylic resin, solvent (IBA), and bentonite paste other than MPS, was kept constant (Table 6).

The dispersions were used in 2K acrylic polyurethane coatings with a PVC value of 13 %. Fresh paint properties are given in Table 7.

In this study, fresh paints were atomized with air pressure and vertically sent to the surface of steel plates. Surface properties of cured films are highly affected by the application viscosity; that is, low viscosity may result in sagging under the influence of gravity and inhomogeneous dry film thickness, whereas high viscosity may lead to a surface defect called orange peeling as a result of quick solvent evaporation and poor leveling. The application viscosity of the studied paint system is 21 seconds at 23 °C, and the application viscosities of the designed samples were kept constant as 21 seconds at 23 °C to ensure similar surface quality. The viscosity of the samples with higher MPS amount was lower, so they required less solvent. Therefore, the amount of volatile organic compounds (VOC) in the formulations was reduced with increasing MPS.

Table 5: TT3 particle size results obtained with various dispersion durations.

Times	15 min	30 min	45 min	90 min	135 min	3 hours	6 hours
D [1,0]	0.472	0.406	0.401	0.347	0.304	0.314	0.302
D [3,2]	0.743	0.678	0.661	0.613	0.537	0.570	0.518
D [4,3]	0.929	0.888	0.844	0.790	0.684	0.720	0.653
D (avg)	0.605	0.596	0.586	0.573	0.546	0.556	0.538
150-250 nm %	1.73	11.74	14.62	31.93	42.50	42.29	42.62
250-350 nm %	43.50	47.45	44.91	37.53	32.15	29.19	32.73
350-990 nm %	51.82	39.06	38.85	29.49	22.78	25.50	22.56

Table 6: Ingredients of dispersions used in white topcoat paints.

Materials	UT	TT1	TT2	TT3	TT4
MPS (g)	0	2.5	5	10	20
IBA (g)	25	25	25	25	25
TiO_2 (g)	100	100	100	100	100
Bentonite paste (g)	11.98	11.98	11.98	11.98	11.98
Acrylic resin* (g)	39.22	39.22	39.22	39.22	39.22
Total (g)	176.2	178.7	181.2	186.2	196.2

* The solid content of acrylic resin is 65 %.

Table 7: Properties of white topcoat paints.

Property (TiO_2/MPS ratio)	UT (100/0)	TT1 (100/2.5)	TT2 (100/5)	TT3 (100/10)	TT4 (100/20)
Solid content, wt. %	61.64	61.83	62.37	63.02	64.80
Solid content, vol. %	47.76	47.99	48.46	48.79	50.21
Viscosity at 23 °C, sec.	85"	82"	77"	70"	58"
Application viscosity at 23 °C, sec.	21"	21"	21"	21"	21"
VOC%	53.5	52.9	52.5	51.8	50.1

The results of topcoats prepared with different MPS amounts, dispersion durations of 30 min and 45 min, and dry film thicknesses of 30 µm and 55 µm are shown in Table 8. Gloss and DoI values decreased with increasing MPS amount, whereas haze values increased. This may be attributed to the microstructures in the film resulting from the self-condensation of silane molecules.

Lightness (L*) and contrast ratio (CR %) correspond to the light scattering efficiency of the coating. These two critical values were compared in detail in Table 9 to underscore the favorable innovation. The highest L* and CR % values were reached with the TT3 sample at 96.83 and 98.55, respectively.

Table 8: White topcoat properties obtained by parametric experiments (PVC:13%).

Sample	Time, min	DFT, µm	L*	a*	b*	CR%	Gloss @ 60°	Gloss @ 20°	Haze	DoI
UT	30	30	94.30	-1.10	-1.03	93.94	95.4	89.5	6.0	97.4
	30	55	96.71	-0.87	0.06	98.13	95.4	90.2	6.5	97.6
	45	30	94.56	-1.11	-1.10	94.94	95.0	90.1	6.7	97.3
	45	55	96.81	-0.87	0.12	98.54	95.9	90.0	6.8	97.5
TT1	30	30	94.49	-1.08	-0.97	94.76	93.7	85.0	6.7	87.7
	30	55	96.81	-0.87	0.18	98.23	93.7	84.7	7.6	71.5
	45	30	94.79	-1.05	-0.83	95.56	93.4	87.6	6.3	91.9
	45	55	96.81	-0.87	0.18	98.47	93.3	87.2	7.7	71.5
TT2	30	30	94.54	-1.07	-0.96	94.28	93.8	86.9	6.7	84.8
	30	55	96.74	-0.90	0.10	98.16	93.8	85.8	7.1	82.9
	45	30	94.65	-1.08	-0.90	95.25	93.8	87.6	6.3	91.0
	45	55	96.54	-0.89	0.07	98.47	94.6	88.7	6.6	89.4

Table 8: Continued.

Sample	Time, min	DFT, µm	L*	a*	b*	CR%	Gloss @ 60°	Gloss @ 20°	Haze	DoI
TT3	30	30	94.64	-1.06	-1.07	94.50	94.6	87.2	6.5	87.2
	30	55	96.83	-0.86	0.08	98.24	94.2	86.8	7.1	76.6
	45	30	94.57	-1.07	-0.96	94.62	94.4	86.2	6.6	77.2
	45	55	96.82	-0.80	0.28	98.55	90.8	84.7	6.9	87.1
TT4	30	30	94.61	-1.05	-1.04	93.81	91.9	80.4	7.9	73.4
	30	55	96.78	-0.84	0.04	98.10	93.3	85.8	7.7	83.5
	45	30	94.46	-1.09	-1.08	95.33	93.5	86.3	7.1	69.1
	45	55	96.70	-0.88	0.13	98.46	93.7	86.4	6.9	86.2

Table 9: Comparison of paint properties for untreated and silane-coupled (100:10 TiO_2 to MPS ratio) pigment samples.

Definition	UT (untreated)	TT3 (TiO_2/MPS ratio: 100/10)
Number of particles in 100 g sample	5.7 E+14	9.2 E+14
Difference from ideal number of particles for max scattering	3.4 E+14	7.0 E+14
Particle percentage between 250-350 nm size, %	34.30	27.40
Amount of paint required for 55 µm & 1 m^2 application, g	101.26	100.40
Amount of pigment in the 55 µm & 1 m^2 application, g	28.81	28.54
Number of particles in the 55 µm & 1 m^2 application	1.6 E+14	2.6 E+14
Amount of pigment required for ideal spacing, g	54.12	33.20
PVC %	12.91	13.05
CPVC %	60.13	60.13
PVC/CPVC	0.215	0.217
L*, 55 µm	96.81	96.83
CR %, 55 µm	98.54	98.55

Furthermore, the relationship between the hiding power and the number of particles for UT and TT3 samples was investigated. It is known that the density of TiO_2 pigment is 4 g/cm^3, and the density change due to silane modification was assumed to be insignificant. The volume of 100 g pigment sample was taken as 25 cm^3, as explained in Section 3.1. The volume fractions of the 25 cm^3 sample were calculated using the volume density. Dividing the calculated volume fractions by the volumes of individual particles, the number of particles at each size class was found. Table 10 is created for 100 g of UT as a sample calculation, and the number of particles was calculated for other samples with the same method. The amount of pigment used to achieve opacity (CR % >98) was 33.20 g for the TT3 silane-modified sample and 54.12 g for the UT untreated sample (Table 9). As a result, 38.6 % less pigment was used in the TT3 sample with 55 µm film thickness compared to the UT sample, and 98.55 % CR was achieved.

Table 10: Calculation of the number of particles in a 100 g of UT dispersion.

Size, µm	Volume Density, %	Volume Fraction	Volume of Particles at the Specified Size, cm^3	Number of Particles at the Specified Size
0.11	0.00	0.00	7.55 E-16	0.00 E+00
0.13	0.07	0.02	1.10 E-15	1.59 E+13
0.15	0.30	0.08	1.63 E-15	4.60 E+13
0.17	0.64	0.16	2.40 E-15	6.68 E+13
0.19	1.04	0.26	3.48 E-15	7.47 E+13
0.21	1.46	0.37	5.13 E-15	7.11 E+13
0.24	1.90	0.48	7.51 E-15	6.32 E+13
0.28	2.33	0.58	1.10 E-14	5.29 E+13
0.31	2.74	0.69	1.62 E-14	4.23 E+13
0.36	3.10	0.78	2.38 E-14	3.25 E+13
0.41	3.45	0.86	3.48 E-14	2.48 E+13
0.46	3.84	0.96	5.10 E-14	1.88 E+13
0.52	4.33	1.08	7.49 E-14	1.45 E+13
0.59	4.97	1.24	1.10 E-13	1.13 E+13
0.68	5.70	1.43	1.61 E-13	8.85 E+12
0.77	6.39	1.60	2.36 E-13	6.76 E+12
0.87	6.96	1.74	3.47 E-13	5.01 E+12
0.99	7.34	1.84	5.10 E-13	3.60 E+12
1.13	7.47	1.87	7.55 E-13	2.47 E+12
1.28	7.34	1.84	1.10 E-12	1.67 E+12
1.45	6.90	1.73	1.60 E-12	1.08 E+12
1.65	6.18	1.55	2.35 E-12	6.57 E+11
1.88	5.24	1.31	3.48 E-12	3.77 E+11
2.13	4.14	1.04	5.06 E-12	2.05 E+11
2.42	3.01	0.75	7.42 E-12	1.01 E+11
2.75	1.95	0.49	1.09 E-11	4.48 E+10
3.12	0.98	0.25	1.59 E-11	1.54 E+10
3.55	0.19	0.05	2.34 E-11	2.03 E+09
4.03	0.03	0.01	3.43 E-11	2.19 E+08
Totals	99.99	25.00		5.66 E+14

3.2.4. Effect of pigment volume concentration

The amount of paint used to cover a particular surface depends on the volumetric solid content. Formulations with higher solid contents, meaning lower VOC, will produce more solid particles in the dry volume. To obtain optimum film properties, PVC should be lower than CPVC in paint formulations. In the experiments carried out to evaluate the effect of silane coupling on white topcoat properties, the PVC/CPVC ratio was found to be close to 0.22 (PVC: 13 %), which is a safe value for the mechanical strength and corrosion resistance of organic coatings.

While the previous sections of the study included experiments with a fixed PVC value of 13 %, the

effects of different PVC values on the topcoat film properties of the UT and TT3 pigment dispersions were investigated in this section. As Diebold indicated that the scattering efficiency of TiO_2 pigments enhances up to a PVC of approximately 15 %, this investigation deliberately maintained PVC levels below this threshold to explore how the scattering contributions of individual TiO_2 particles are affected by lower PVC values [29]. Topcoat formulations of UT and TT3 pigment dispersions were prepared with three different PVC. As PVC increases, more particles are packed in a fixed volume, and interparticle distance decreases. The light scattering ability of TiO_2 pigments in dry films is primarily influenced by the refractive index contrast between the TiO_2 particles and their surroundings and the spatial arrangement (proximity) of the TiO_2 particles. While the refractive index of TiO_2 remains constant, the average refractive index of the surroundings is affected by the volume concentration of TiO_2, thereby impacting the light scattering efficiency of the TiO_2. As PVC increases to a certain extent, more TiO_2 particles occupy the same fixed volume, resulting in a higher refractive index of the coating and diminished light scattering efficiency due to the increased density of the pigment phase. PVC levels ≤13 % (7, 11, and 13 %) were chosen to prevent interference of particles with each other and reduction of the scattering efficiency below the 400 nm spacing [29-30].

Topcoat film properties of the UT and TT3 pigment dispersions with 13 % and lower PVC were presented in Table 11. Lightness (L*), contrast ratio (CR%), gloss, haze, and DoI values were compared concerning PVC and film thickness. It was observed that the TT3 samples were superior to the UT samples in terms of hiding power and lightness. The L* and CR% values for TT3 with 7, 11, and 13 % PVC were higher than those of the UT samples (Figure 6). The differences were more significant at lower PVC values and lower film thicknesses. On the other hand, the change in gloss, haze, and DoI for all measurements were less pronounced (Table 11).

Table 11: Topcoat film properties of the UT and TT3 pigment dispersions with different PVC values.

Sample	PVC	DFT. µm	L*	CR%	Gloss. @60°	Gloss. @20°	Haze	DoI
UT	7	30	92.01	90.05	95.0	89.6	5.4	98.0
	7	55	95.61	95.98	95.8	90.4	6.1	98.5
	11	30	93.11	91.81	95.0	89.2	5.8	97.8
	11	55	96.12	96.60	95.9	90.2	6.1	98.6
	13	30	94.30	93.94	95.4	89.5	6.0	97.4
	13	55	96.47	97.15	95.7	89.9	6.3	97.8
TT3	7	30	92.82	90.45	95.2	89.4	5.5	96.4
	7	55	95.50	96.08	95.4	89.2	5.9	96.2
	11	30	94.26	94.33	95.5	89.2	6.1	93.9
	11	55	96.49	98.14	96.0	89.4	6.4	95.2
	13	30	94.64	94.50	94.6	87.2	6.5	87.2
	13	55	96.82	97.33	95.9	89.3	6.6	91.7

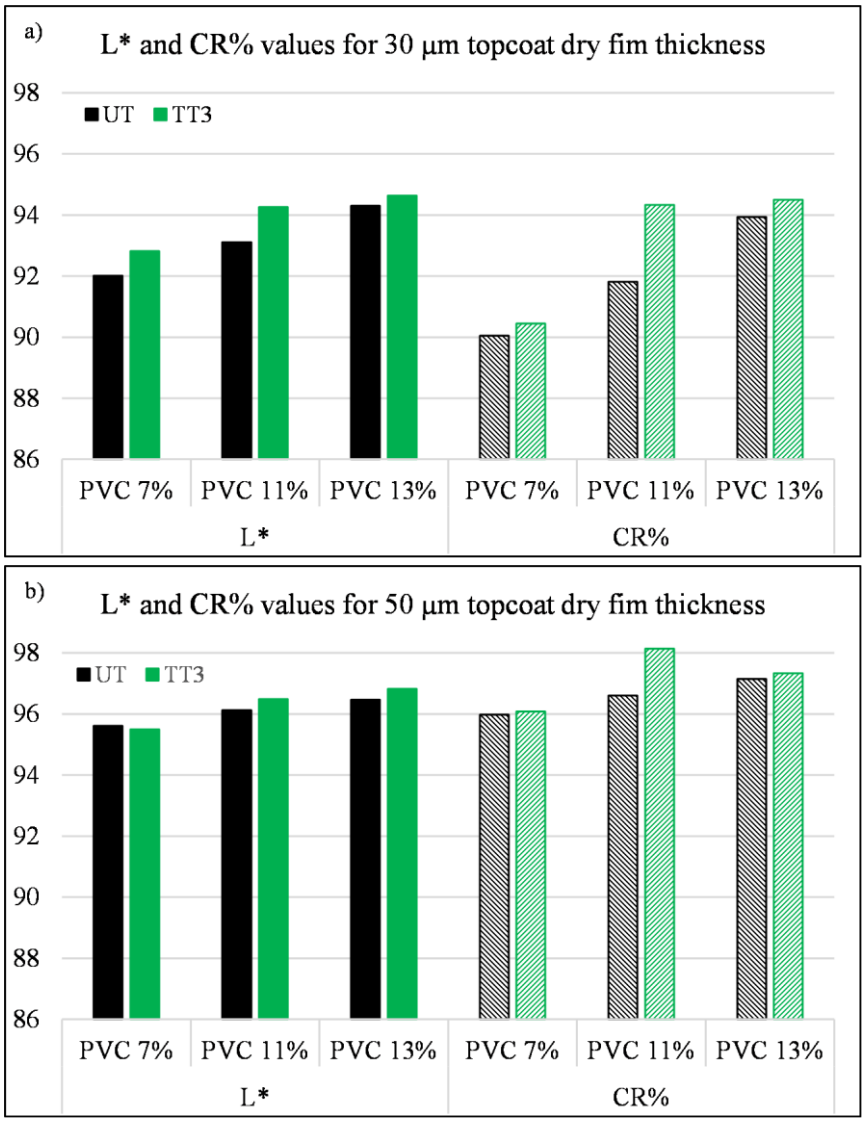

Figure 6: Effect of PVC on lightness and contrast ratio of the topcoats containing UT and TT3 dispersions at a) 30 µm and b) 55 µm dry film thickness.

When topcoats containing UT and TT3 dispersions were evaluated separately, lower PVC levels at a given film thickness allowed for wider spacing between pigment particles in dry films based on the lower L* and CR % values obtained. With the increase of PVC, the number of particles interacting with light increases, but the scattering efficiency of an individual particle decreases due to crowding. Dilution of pigment concentration promotes light scattering by a single particle, but fewer number of particles results in decreased total scattering. The lightness values of the samples UT and TT3 of 7 % PVC at 30 µm film thickness were 92.01 and 92.82, respectively. However, those were 93.11 and 94.26 for UT and TT3 at 30 µm with 11 % PVC. Similarly, the lightness values of the samples UT and TT3 at 30 µm film thickness increased to 94.30 and 94.64, respectively, as the topcoats were formulated with 13 % PVC. A similar increase is observed when the lightness values measured at 55 µm film thickness for the samples UT and TT3 are reviewed. Considering the increase in lightness values, the tendency of TT3-treated pigments to crowd is less pronounced, thanks to the steric hindrance the MPS coupling provides. A similar conclusion can be drawn when the increase in contrast ratios is considered. It was further concluded that the MPS-grafted pigments were evenly distributed within the film as the change in gloss, haze, and DoI is similar at both dry film thicknesses for

UT and TT3 pigmented topcoats of 30 and 50 μm.

3.2.5. Investigation of pigment crowding with SEM images

Lateral sections of the white topcoat films were investigated and compared using SEM micrographs focusing on flocculation and crowding of pigment particles. Figure 7 shows the images of UT, TT3, and TT4 topcoats with 13 % PVC, examining the TiO_2/MPS ratio of 100/0, 100/10, and 100/20, respectively. TT3 topcoat with 11 % PVC, expressed as TT3*, was additionally evaluated together with TT3 topcoat with 13% PVC to observe the effect of PVC.

SEM micrographs at 5000× magnification in Figure 7 qualitatively show the relative spatial distribution of pigment particles within the acrylic medium [31]. The white parts in the images are TiO_2 particles, whereas the grey parts are acrylic medium [32]. Figure 7a reveals the more pronounced random distribution of the untreated TiO_2 with local flocculates. MPS-grafted pigment particles (Figure 7b, Figure 7c, and Figure 7d) were more evenly distributed in the organic coating than the untreated pigment particles (Figure 7a). Also, 11 % PVC resulted in larger gaps between pigment particles than 13 % PVC, as expected, since the same pigment was diluted within the fixed volume.

3.2.6. Effect of silane coupling and PVC level on corrosion resistance

The samples of UT (PVC: 13 %), TT3 (PVC: 13 %), and TT3* (PVC: 11 %) white topcoats were subjected to a corrosive environment for 1000 h. Three plates with an X-cut on the dry film were prepared and tested for each sample. The degree of blistering was classified according to ASTM D714 standard where the medium, medium dense, and dense frequency of blisters are designated as M, MD, and D, respectively, and numerical size scales from 10 to 0, in which No. 10 represents no blistering and No. 8 is the smallest size blister seen by the unaided eye. Rust widths were also measured with a ruler after scratching them with a paint remover (Table 12). Images of the plates (Figure 8) after the test period showed that the blister formation and rust widths of the MPS-grafted pigmented and reduced PVC topcoat samples were similar to those of the untreated pigmented topcoat samples. Therefore, it was concluded that the MPS grafting does not adversely affect the corrosion resistance of coating films.

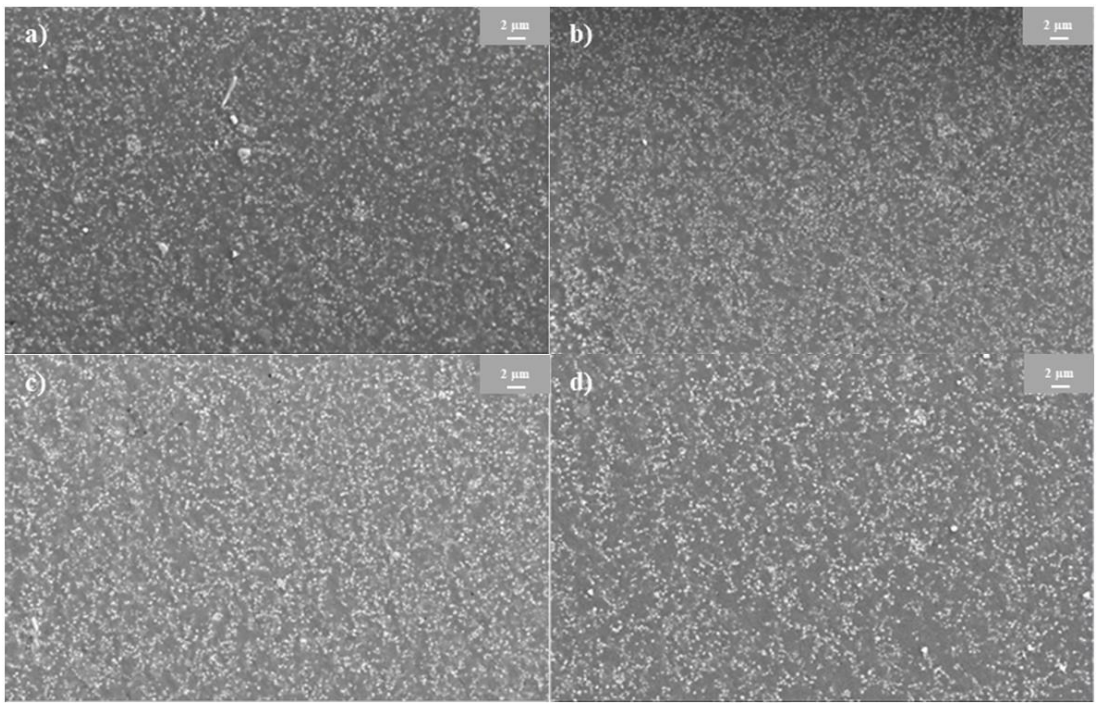

Figure 7: SEM micrographs of a) UT (PVC:13%), b) TT3 (PVC:13%), c) TT4 (PVC:13%), and d) TT3* (PVC:11%) topcoat lateral sections at 5000× magnification.

Table 12: Comparison of corrosion progression after 1000 hours of salt spray test.

Samples	1000 h test results		Corrosion Progression	
	General area	X. cross area	Rust width. mm	Average. mm
3×UT (PVC:13%)	8MD	4D	5.50; 5.25; 3.50	4.75
3×TT3 (PVC:13%)	8D	4M	3.62; 5.12; 4.62	4.45
3×TT3* (PVC:11%)	8M	4D	4.12; 3.75; 5.50	4.46

Figure 8: Corrosion progression after salt spray test for the coated plates. Top: UT (PVC: 13%), Middle: TT3 (PVC: 13%), and Bottom: TT3* (PVC: 11%).

4. Conclusions

This study aimed to develop a method to prevent the crowding of TiO_2 pigment particles to increase the light scattering efficiency in white automotive topcoats. 3-methacryloxypropyltrimethoxysilane (MPS) was hydrolyzed in isobutyl alcohol (IBA) and grafted onto pigment particles during dispersion in acrylic medium to ensure proper spacing between particles when formulated in topcoat paints to provide desired surface properties. Untreated (UT) and MPS-coupled TiO_2 particles were characterized using FTIR and TGA techniques, and the highest grafting efficiency was revealed for the TiO_2 to MPS mass ratio of 100/10 (TT3). Dispersion time was optimized for the TT3 sample, and the highest number of particles within 250-350 nm, the most efficient light scattering size range, was obtained with 30- and 45-minute dispersion processes. Besides the TT3 dispersion, the UT dispersion and dispersions of different TiO_2 to MPS mass ratios were used in the white topcoat formulations and spray applied onto steel plates to give 30 µm and 55 µm dry film thicknesses with 13% pigment volume concentration (PVC). Color, hiding power, and surface properties of the topcoats with the two film thicknesses revealed the favorable use of the TT3 pigment dispersion with negligible loss in gloss, haze, and distinctness of image, especially the high lightness and contrast ratio values of this dispersion made it the opaquest topcoat paint. The effect of PVC on the pigment spacing was investigated with topcoats of 7, 11, and 13 % PVC, using UT and TT3 dispersions. The results showed that lower PVC levels enable a wider spacing between pigment particles in dry films. It was further revealed that the UT dispersion tended to exhibit more pigment crowding with the same PVC as the TT3 dispersion, whereas an increase in PVC did not reduce hiding power and lightness values, thus the evenly pigment distribution in dry film with the TT3 dispersion. The spatial distribution of pigment particles in dry films, as shown in SEM micrographs, is consistent with this conclusion. The silane coupling approach could be applied to other pigments and pigmented coating systems beyond acrylic topcoats pigmented solely with TiO_2. Depending on the usage area and the durability expectations, studying silane coupling in different resin

environments would certainly be a direction that could be evaluated. External durability testing is planned with the acrylic white topcoats created in this study, and the authors encourage researchers to ensure weathering resistance for future silane coupling studies using different pigments or resins. As in topcoats colored with multiple types of pigments, the absorption and reflection contributions of individual pigment chemistries in the visible light spectrum provide much better opacity; therefore, this study intentionally focused on TiO_2 as hiding power is a critical issue in white topcoats. The same hiding power was achieved with lower PVC levels at a given film thickness and lower film thicknesses with a given PVC using a smaller amount of the TT3 dispersion than the untreated TiO_2 dispersion. Hence, it was proven that the same surface hiding was obtained using less pigment in coatings with the MPS-coupled TiO_2 particles. The TT3-containing topcoat paint formulation also required less volatile organic compounds (VOCs) to achieve application viscosity and to ensure surface quality. Using lower topcoat film thicknesses to cover unit area with silane coupling reduces paint consumption and leads to reduced VOC emissions into the environment. Hence, the commercialization potential of this study is substantial, as the paint manufacturers are constantly seeking environment-friendliness and sustainability. However, one should be prepared for potential challenges when planning the industrial scalability of MPS grafting onto TiO_2 pigments. Achieving uniform silanization might be a challenge across large batches as temperature and mixing intensity variations can lead to inconsistent hydrolysis and condensation. Also, using zirconium beads may need adjustment in scale-up scenarios as larger volumes may require different bead sizes or configurations to maintain effective energy transfer for dispersion. It should not be forgotten that quality control assessment of particle size distribution and silane coupling in large batches is essential to maintain the desired performance of the end product.

Acknowledgments

Kansai Altan Boya Sanayi A.Ş. kindly provided the resources for the experimental phase of this research, and the authors are thankful to Prof. Dr. Günseli Özdemir, whose invaluable academic guidance and insightful suggestions greatly contributed to the success of this research.

5. References

1. Brock T, Groteklaes M, Mischke P. European coatings handbook. Hannover: Vincentz; 2000.
2. Wicks Jr ZW, Jones FN, Pappas SP. Organic coatings: Science and technology. 3rd ed. Hoboken (NJ): Taylor & Francis; 2007.
3. Diebold MP. Application of light scattering to coatings: A user's guide. London: Springer; 2014.
4. Titanium dioxide for coatings [product overview]. The Chemours Company; 2019. Available from: https://www.tipure.com/en/-/media/files/tipure/legacy/titanium-dioxide-for-coatings.pdf
5. Diebold MP, Monte Carlo A. determination of the effectiveness of nanoparticles as spacers for optimizing TiO_2 opacity. J Coat Technol Res. 2011; 8(5): 541-552. doi:10.1007/s11998-011-9342-1
6. Thiele ES, French RH. Light-scattering properties of representative, morphological rutile titania particles studied using a finite-element method. J Am Ceram Soc. 1998;81(3):469-479. doi:10.1111/j.1151-2916.1998.tb02364.x.
7. Löf D, Hamieau G, Zalich M, Ducher P, Kynde S, Midtgaard SR, et al. Dispersion state of TiO_2 pigment particles studied by ultra-small-angle X-ray scattering revealing dependence on dispersant but limited change in drying of paint coating. Prog Org Coat. 2020; 142: 1-8. https://doi.org/10.1016/j.porgcoat.2020.105590.
8. Lambourne R, Strivens TA. Paint and surface coatings: Theory and practice. 2nd ed. Cambridge: Woodhead Publishing Ltd; 1999.
9. Uzunkavak O, Özdemir G. Design of dark-colored acrylic coatings for increased LiDAR detection in autonomous vehicles. Prog Org Coat. 2024; 196: 1-11. https://doi.org/10.1016/j.porgcoat.2024.108756.
10. Yebra DM, Weinell CE. Key issues in the formulation of marine antifouling paints. In: Hellio C, Yebra DM. (eds.) Advances in marine antifouling coatings and technologies. Cambridge: Woodhead Publishing Ltd; 2009. 308-333.
11. Tyler F. Tailoring TiO_2 treatment chemistry to achieve desired performance properties [internet]. PCI Magazine; 2000. Available from: https://www.pcimag.com/articles/86202-tailoring-tio2-treatment-chemistry-to-achieve-desired-performance-properties.
12. Buxbaum G, Pfaff G. Industrial inorganic pigments. 3rd ed. Weinheim: Wiley-VCH; 2005.
13. Arkles B. Tailoring surfaces with silanes. Chem

Tech. 1977; 7(12): 766-778.
14. Plueddemann EP. Silane coupling agents. 2nd ed. New York: Plenum Press; 1991.
15. Tesoro G, Wu Y. Silane coupling agents: The role of the organofunctional group. J Adhesion Sci Technol. 1991; 5(10): 771-784. https://doi.org/10.1163/156856191X00206.
16. Sideridou ID, Karabela MM. Effect of the amount of 3-methacryloxypropyltrimethoxysilane coupling agent on physical properties of dental resin nanocomposites. Dent Mater. 2009; 25: 1315-1324. https://doi.org/10.1016/ j.dental.2009.03.016.
17. Siddiquey IA, Ukaji E, Furusawa T, Sato M. The effects of organic surface treatment by methacryloxypropyltrimethoxysilane on the photostability of TiO_2. Mater Chem Phys. 2007;105:162-168. https://doi. org/10.1016/j.matchemphys.2007.04.017.
18. Sabzi M, Mirabedini SM, Zohuriaan-Mehr J, Atai M. Surface modification of TiO_2 nanoparticles with silane coupling agents and investigation of its effect on the properties of polyurethane composite coating. Prog Org Coat. 2009; 65: 222-228. https://doi.org/10.1016/j.porgcoat.2008.11.006
19. Zhao J, Milanova M, Warmoeskerken MMCG, Dutschk V. Surface modification of TiO_2 nanoparticles with silane coupling agents. Colloids Surf A: Physicochem Eng Aspects. 2012;413:273-279. https://doi.org/10.1016/j.colsurfa.2011.11.033.
20. A guidebook to particle size analysis [internet]. Horiba Instruments Inc.; 2012. Available from: https://ats-scientific.com/uploads/PSA_Guidebook.pdf
21. International Organization for Standardization. ISO 7724-3. Paints and varnishes - Colorimetry - Part 3: Calculation of colour differences. Geneva: ISO; 1984.
22. American Society for Testing and Materials. ASTM B117 – 19. Standard Practice for Operating Salt Spray (Fog) Apparatus. West Conshohocken (PA): ASTM International; 2019.
23. American Society for Testing and Materials. ASTM D714-02. Standard Test Method for Evaluating Degree of Blistering of Paints. West Conshohocken (PA): ASTM International; 2017.
24. Larkin PJ. IR and Raman spectroscopy: Principles and spectral interpretation. San Diego: Elsevier Inc.; 2011.
25. Fei X, Cao L, Liu Y. Modified C.I. pigment red 170 with a core-shell structure: Preparation, characterization and computational study. Dyes Pigm. 2016; 125: 192-200. https://doi.org/10.1016/j.dyepig.2015.10.021.
26. Florea NM, Lungu A, Vasile E, Iovu H. The influence of nanosilica functionalization on the properties of hybrid nanocomposites. High Perform Polym. 2012; 25(1): 61-69. https://doi.org/10.1177/0954008312455831.
27. Liu Q, Ding J, Chambers DE, Debnath S, Wunder SL, Baran GR. Filler-coupling agent-matrix interactions in silica/polymethylmethacrylate composites. J Biomed Mater Res. 2001; 57(3): 384-393. https://doi.org/10.1002/1097-4636(20011205)57:3%3C384::aid-jbm1181%3E3.0.co;2-f.
28. Cheng Q, Li C, Pavlinek V, Saha P, Wang H. Surface-modified antibacterial TiO_2/Ag^+ nanoparticles: Preparation and properties. Appl Surf Sci. 2006; 252(12): 4154-4160. https://doi.org/10.1016/j.apsusc.2005.06.022.
29. Diebold M, Kwoka R, Mukoda D. TiO_2 scattering optimization and not-in-kind opacity alternatives. J Coatings Tech. 2013; 10(2): 30-35.
30. Song GY, Jang I, Jeon SW, Ahn SH, Kim JY, Sa G. Controlling the surface properties of TiO_2 for improvement of the photo-performance and color uniformity of the light-emitting diode devices. J Ind Eng Chem. 2021; 94:180-187. https://doi.org/10.1016/j.jiec.2020.10.031.
31. Lin JC, Heeschen W, Reffner J, Hook J. Three-dimensional characterization of pigment dispersion in dried paint films using focused ion beam-scanning electron microscopy. Microsc Microanal. 2012; 18(2):266-271. https://doi.org/10.1017/S1431927611012 44X.
32. Yang F, Chen B, Hashimoto T, Zhang Y, Thompson G, Robinson I. Investigation of three-dimensional structure and pigment surrounding environment of a TiO_2 containing waterborne paint. Materials. 2019; 12(3): 464-475. doi:10.3390/ma12030464.

How to cite this article:
Ödev A, Uzunkavak O. Prevention of TiO_2 Crowding through Steric Hindrance by Silane Coupling in Organic Coatings. Prog Color Colorants Coat. 2025;18(3):343-361. https://doi.org/10.30509/pccc.2025.167429.1345.